

Published in final edited form as:

Atherosclerosis. 2012 August ; 223(2): 365–371. doi:10.1016/j.atherosclerosis.2012.05.023.

Plaque characteristics and arterial remodeling in coronary and peripheral arterial systems

Yoshiki Matsuo, MD, PhD^{*}, Takuro Takumi, MD, PhD^{*}, Vergheze Mathew, MD^{*}, Woo-Young Chung, MD, PhD^{*}, Gregory W. Barsness, MD^{*}, Charanjit S. Rihal, MD^{*}, Rajiv Gulati, MD^{*}, Eric T. McCue, RCIS^{*}, David R Holmes, MD^{*}, Eric Eeckhout, MD[†], Ryan J. Lennon, MS[‡], Lilach O. Lerman, MD, PhD[§], and Amir Lerman, MD^{*}

^{*}the Division of Cardiovascular Disease, Mayo Clinic, Rochester, Minnesota, USA [‡]the Division of Biomedical Statistics and Informatics, Mayo Clinic, Rochester, Minnesota, USA [§]the Division of Nephrology and Hypertension, Mayo Clinic, Rochester, Minnesota, USA [†]The Cardiology Division, Centre Hospitalier Universitaire Vaudois, Lausanne, Switzerland

Abstract

Background—Few studies have examined plaque characteristics among multiple arterial beds in vivo. The purpose of this study was to compare the plaque morphology and arterial remodeling between coronary and peripheral arteries using gray-scale and radiofrequency intravascular ultrasound (IVUS) at clinical presentation.

Methods and Results—IVUS imaging was performed in 68 patients with coronary and 93 with peripheral artery lesions (29 carotid, 50 renal, and 14 iliac arteries). Plaques were classified as fibroatheroma (VH-FA) (further subclassified as thin-capped [VH-TCFA] and thick-capped [VH-ThCFA]), fibrocalcific plaque (VH-FC) and pathological intimal thickening (VH-PIT). Plaque rupture (13% of coronary, 7% of carotid, 6% of renal, and 7% of iliac arteries; P=NS) and VHTCFA (37% of coronary, 24% of carotid, 16% of renal, and 7% of iliac arteries; p=0.02) were observed in all arteries. Compared with coronary arteries, VH-FA was less frequently observed in renal (p<0.001) and iliac arteries (p<0.006). Lesions with positive remodeling demonstrated more characteristics of VH-FA in coronary (84% vs. 25%, p<0.001), carotid (72% vs. 20%, p=0.001), and renal arteries (42% vs. 4%, p=0.001) compared with those with intermediate/negative remodeling. There was positive relationship between RI and percent necrotic area in all four arteries.

Conclusions—Atherosclerotic plaque phenotypes were heterogeneous among four different arteries; renal and iliac arteries had more stable phenotypes compared with coronary artery. In contrast, the associations of remodeling pattern with plaque phenotype and composition were similar among the various arterial beds.

© 2012 Elsevier Ireland Ltd. All rights reserved.

Corresponding author: Amir Lerman, MD., lerman.amir@mayo.edu, Division of Cardiovascular Disease, Mayo Clinic, 200 First Street SW, Rochester, Minnesota 55905, U.S.A., Tel: 507-255-4152 Fax: 507-255-2550.

Publisher's Disclaimer: This is a PDF file of an unedited manuscript that has been accepted for publication. As a service to our customers we are providing this early version of the manuscript. The manuscript will undergo copyediting, typesetting, and review of the resulting proof before it is published in its final citable form. Please note that during the production process errors may be discovered which could affect the content, and all legal disclaimers that apply to the journal pertain.

Disclosures: None

Keywords

atherosclerosis; intravascular ultrasound; plaque morphology; peripheral artery disease; coronary artery disease

1. Introduction

Atherosclerosis is a systemic process with manifestations in multiple arterial beds. Given the rising prevalence of peripheral artery disease (PAD) [1], understanding differences in plaque characteristics and clinical presentation may have implications for treatment and prevention of cardiovascular disease.

A previous postmortem study showed that foam cell lesions and lipid core plaques were highly prevalent in coronary and carotid arteries, while fibrous plaques dominated severe atherosclerosis in femoral arteries [2]. However, few studies have compared plaque characteristics in multiple arterial beds in vivo. We have recently reported a comparative analysis of atherosclerotic plaques between the coronary and the renal arterial beds [3]. The purpose of this study was to extend those previous observations and to test the hypothesis that there is a heterogeneous manifestation of atherosclerosis in different human arterial beds. In order to address our hypothesis we compared plaque morphology and arterial remodeling between coronary and peripheral arteries using gray-scale and radiofrequency intravascular ultrasound.

2. Methods

2.1 Patients

The Mayo Clinic Institutional Review Board approved this study protocol. Between May 2008 and June 2011, 256 interventional and diagnostic IVUS for left main coronary artery (LMCA) and peripheral arteries (carotid artery, renal artery, and iliac artery) were performed for clinical purposes. The decision to perform IVUS examination was based on the discretion of the operator. Seventy-eight patients with LMCA lesions, 34 with extracranial internal carotid artery (ICA) lesions, 66 with renal lesions and 18 with iliac lesions, met the following criteria: 1) atherosclerotic stenotic lesions in at least any one of LMCA, ICA, main renal arteries or iliac arteries; and 2) adequate image quality. Patients were excluded if they had 1) restenosis lesions (12 renal and 2 iliac lesions); 2) ostial and bifurcation lesions with image distortion due to non-coaxial IVUS transducer position (3 LMCA, 2 ICA and 2 renal lesions); 3) lesions without reliable reference segments (7 LMCA lesions and 2 renal lesions); 4) lesions with extensive calcification that limit the quantitative assessment of vessel area [4] (3 ICA and 2 iliac lesions), and 5) lesions with angiographically determined thrombus (2 LMCA lesions). A total of 161 lesions (68 LMCA, 29 ICA, 50 renal, and 14 [9 common and 5 external] iliac artery lesions) from 161 patients were included. Clinical characteristics including coronary risk factors were investigated. Hypertension was defined as systolic blood pressure ≥ 140 mm Hg, diastolic blood pressure ≥ 90 mm Hg, or use of anti-hypertensive drugs. Dyslipidemia was defined as a present or past history of low-density lipoprotein cholesterol level ≥ 130 mg/dl, HDL <40 mg/dl, total cholesterol ≥ 200 mg/dl, or triglycerides ≥ 150 mg/dl. Serum creatinine and fasting lipid levels were measured before the angiographic procedure.

2.2 Images Acquisition

Angiography was performed followed by both gray-scale and virtual histology intravascular ultrasonography (VH-IVUS). All patients received intravenous heparin (100 U/kg) before

the procedure. After intraarterial administration of 100–200 µg of nitroglycerin, IVUS was performed with a phased-array 20 MHz IVUS catheters and the S5 Imaging System (Eagle-Eye Gold, Volcano Corporation, Rancho Cordova, California). After the IVUS catheter was advanced distally beyond the lesion over a guidewire under fluoroscopic control, manual pullback was used for the IVUS catheter. The gray-scale IVUS and captured radiofrequency data were recorded onto a DVD-R and analyses were performed offline using dedicated software [5].

2.3 IVUS Image Analyses

Images were interpreted offline by two experienced observers blinded to baseline patient characteristics in an IVUS Imaging center at our institution as previously described [3,6]. Analysis of the medial-advitial and luminal borders in each analyzable cross-sectional frame for the entire pullback length was performed by IVUS core laboratory personnel. Two commercial software (IVUSLab software and pcVH 2.2, Volcano Corporation, Rancho Cordova, California) were used to reconstruct IVUS B-mode images from the radiofrequency data and to calculate geometric and composition data for each IVUS frame. The target lesion site image slice was the slice with the smallest lumen cross sectional area (CSA). If there were several slices with equal lumen CSA, the one with the largest external elastic membrane (EEM) area and plaque CSA was analyzed [4]. Automatically detected lumen and vessel border contours were manually corrected. A reference image slice was selected as the most normal-looking cross section distal or proximal to the target lesion without any intervening large side branch. At each image slice, EEM, lumen CSA, and plaque plus media (P+M) CSA were measured. The plaque burden was calculated as P+M CSA divided by EEM CSA. Remodeling of target lesion was determined using the remodeling index (RI), calculated as the EEM area of the target lesion site divided by that of the reference site. Positive remodeling (PR) was defined as a $RI \geq 1.05$ and intermediate/negative remodeling (IR/NR) as an $RI < 1.05$. Plaque rupture was defined as the presence of a cavity that communicated with the lumen with an overlying residual fibrous cap fragment [7]. Composition data were color-coded as follows: fibrous tissue (dark green areas), fibrofatty tissue (light-green areas), necrotic core (red areas), and dense calcium (white areas). Interobserver and intraobserver variability of IVUS data were shown elsewhere [3].

2.4 Plaque Classification

We utilized the following plaque classifications according to previously published VH-IVUS classifications [8]: 1) Fibroatheroma (VH-FA): plaque burden >40%, confluent necrotic core >10% plaque cross-sectional area, all for 3 consecutive frames. 2) Thin-capped fibroatheroma (VH-TCFA): fibroatheroma with the confluent necrotic core (>10% of plaque cross-sectional area) in contact with vessel lumen for 3 consecutive frames. 3) Thick-capped fibroatheroma (VHThCFA): fibroatheroma (>10% of confluent necrotic core for 3 consecutive frames) not fulfilling VH-TCFA conditions. 4) Fibrocalcific plaque (VH-FC): plaque with dense calcium >10% plaque cross-sectional area in 3 consecutive frames, not meeting VH-FA definition. 5) Pathological intimal thickening (VH-PIT): plaque not meeting VH-FA or VH-FC definitions and predominantly fibrous tissue.

2.5 Statistical Analysis

Continuous variables were presented as mean \pm SD and categorical variables were expressed as frequencies. For continuous variables, one-way analysis of variance (ANOVA) or Kruskal-Wallis test (in case of skewed data) were used for multiple comparisons among groups. For categorical variables, comparisons were performed using chi-square statistics. If a significant difference was found with ANOVA, Kruskal-Wallis or chi-square test, a post hoc multiple comparisons between coronary artery and each peripheral artery were performed using Dunnett's test or Steel-Dwass test for continuous variables and Bonferroni

correction for categorical variables. The correlation between RI and plaque components was evaluated by Spearman's rank correlation analysis. Statistical analysis was performed with JMP version 9.0 (SAS Institute, Cary, North Carolina). A value of $P < 0.05$ for initial assessment was considered significant. In post hoc analysis, P values < 0.016 were considered statistically significant.

3. Results

3.1 Clinical Characteristics

Table 1 shows clinical characteristics and laboratory data of our patients. Eleven (16%) patients with coronary artery disease presented with acute coronary syndrome and 57 (84%) presented with stable angina. Five patients (17%) with carotid artery disease had symptomatic stenosis and 24 (83%) had asymptomatic stenosis. All patients with carotid artery disease had been diagnosed with stenosis greater than or equal to 70% by carotid duplex ($n=16$), magnetic resonance angiography ($n=11$), or computed tomography angiography ($n=3$) prior to catheterization and they were planned for carotid artery stenting. Thirty five (70%) patients with renal artery disease had refractory hypertension and 6 (12%) had unexplained renal failure and 9 (18%) had a history of flash pulmonary edema. All patients with iliac artery disease had chronic lower extremity ischemia. According to the Rutherford classification [9], 4 (29%) patients were graded as category 0, 1 (7%) as category 1, 4 (29%) as category 2, 5 (36%) as category 3, none as category 4 and 5. IVUS was used as an adjunct to subsequent catheter intervention in 6 (9%) patients with coronary, 29 (100%) with carotid, 45 (90%) with renal, and 7 (50%) with iliac artery disease. In the other cases, IVUS was used to make another therapeutic decision such as surgery or medical treatment.

3.2 Angiographic and IVUS findings

IVUS gray-scale parameters were shown in Table 2. Plaque ruptures were demonstrated (Appendix A) in all the arteries.

3.3 Plaque Phenotype and Composition

The distribution of plaque phenotypes assessed by VH-IVUS (Appendix B) was different in the four arterial beds ($p < 0.001$, Figure 1). Compared with coronary artery, carotid artery plaques did not show significant difference ($p=0.53$). Plaques demonstrated less characteristics of VH-FA in renal ($p < 0.001$) and iliac arteries ($p=0.006$) compared with coronary arteries. Renal arteries had the highest prevalence of VH-PIT (43%) and the lowest prevalence of VH-FC (18%). In iliac arteries, half of the plaques (50%) were VH-FC.

The percent area occupied by each plaque component at the minimal lumen site was shown in Figure 2. Significant differences were observed in the percent area of necrotic core ($p < 0.001$) and dense calcium ($p=0.002$) in the four arteries.

3.4 Plaque Characteristics and Remodeling Pattern

The distribution of plaque phenotypes was different between PR and IR/NR groups in coronary ($p < 0.001$), carotid ($p=0.01$), renal ($p=0.01$) and iliac arteries ($p=0.04$) (Figure 3). Compared with lesions with IR/NR, those with PR demonstrated more characteristics of VH-FA in coronary ($p < 0.001$), carotid ($p=0.001$) and renal arteries ($p=0.001$). Similar observations were made regarding VH-TCFA (coronary; $p=0.01$, carotid; $p=0.04$, and renal arteries; $p=0.02$). In iliac arteries, more than half (64%) of IR/NR lesions were VH-FC. With regard to plaque composition, PR lesions had greater percent necrotic core area than IR/NR lesions ($16 \pm 5\%$ vs. $10 \pm 5\%$, $p < 0.05$) in coronary arteries.

There was a positive linear relationship between RI and percent necrotic core area in coronary arteries ($r=0.26$, $p=0.03$). No relationship was observed between RI and other plaque components in coronary arteries (fibrous tissue; $r=-0.51$, $p=0.68$, fibrofatty tissue; $r=-0.93$, $p=0.45$, dense calcium; $r=-0.12$, $p=0.32$). Similarly, RI were correlated with percent necrotic core area ($r=0.40$, $p=0.03$) but not with the other components (fibrous tissue; $r=0.23$, $p=0.22$, fibrofatty tissue; $r=-0.33$, $p=0.08$, dense calcium; $r=-0.18$, $p=0.35$) in carotid, renal (necrotic core; $r=0.41$, $p=0.003$, fibrofatty tissue; $r=-0.38$, $p=0.01$ and fibrous tissue; $r=0.21$, $p=0.14$, dense calcium; $r=0.19$, $p=0.19$) and iliac arteries (necrotic core; $r=0.66$, $p=0.01$ and fibrous tissue; $r=-0.04$, $p=0.91$, fibrofatty tissue; $r=-0.47$, $p=0.09$, dense calcium; $r=0.29$, $p=0.32$). Thus, in all four arterial beds, there was a significant correlation between the necrotic core and RI.

3.5 Gender Difference

Plaque morphology was compared in each arterial bed according to gender (Appendix C). In coronary artery, women had smaller EEM CSA both in lesion site ($p=0.008$) and reference segment ($p=0.006$) and had tendency to have less plaque rupture ($p=0.19$). In carotid artery, women had smaller plaque burden than men ($p=0.03$). Remodeling index in women was higher than men in carotid artery ($p=0.007$) and tended to be higher in renal artery ($p=0.12$). There was no statistical difference regarding plaque phenotype and composition assessed by VH-IVUS (Appendix D).

4. Discussion

The present in vivo study demonstrates for the first time that there are artery-specific differences in atherosclerotic plaque phenotype and composition, as well as similarities in the association of plaque remodeling with plaque components in four different arterial beds. Such heterogeneity in plaque composition may explain the differential clinical presentation of atherosclerosis in different arterial beds.

VH-FAs were relatively infrequently observed in renal and iliac arteries where stable plaque phenotypes such as VH-PIT and VH-FC were more often observed. These observations were in agreement with previous histological studies [2]. However, as apposed to previous studies, our data was based on the IVUS finding for the target lesions and the distribution of plaque phenotype was linked to clinical presentations of our patients. Thus, the current study extends these previous in vitro observations and confirmed these findings in vivo. Clinical manifestations are determined not only by the degree of obstructive atherosclerosis but also local and regional end-organ damage of the arterial territories. The primary pathophysiological mechanism in coronary and carotid arteries is atherothrombosis such as myocardial infarction or stroke. On the other hand, it is presumed that hypoperfusion is the predominant mechanism in renal artery disease. In our study subjects with renal artery disease, the predominant plaque phenotype at clinical presentation was VH-PIT (56%). Yet, intriguingly, 6% showed plaque rupture and 16% had VH-TCFA. These findings imply that atherothrombosis in renal artery might also play a role in the pathophysiology of hypertension and end-stage renal disease, although further studies are required. Most iliac artery diseases also manifested as stable phenotypes in this study subjects. However, Okura et al. [10] demonstrated that plaque ruptures in ilio-femoral lesion were observed in patients presenting with acute coronary syndrome. Hence, the plaque phenotypes could depend on patients' clinical status in peripheral artery disease as well.

There are a number of possible explanations for the heterogeneity of plaque phenotype. The underlying arterial structure could have a potential influence. The LMCA, proximal ICA, proximal renal artery and external iliac artery involve a transitional zone between elastic and muscular artery types [11,12], which are prone to foam cell lesions and lipid cores. In

addition, the underlying differences in hemodynamics such as non-uniform distribution and higher time-dependent wall shear rate in carotid compared with femoral arteries [13] might be etiologic [14]. Genetically, variable gene expression was demonstrated to be associated with plaque development and progression [15]. Moreover, higher density of vasa vasorum, a key factor in plaque destabilization [16], was demonstrated in human coronary arteries compared with renal and femoral arteries [17]. Thus, a complex and multifactorial pathophysiological process may explain in part the heterogeneity on atherosclerosis in different arterial beds.

The present study shows the association of remodeling pattern with plaque phenotype and composition. These results extended findings of previous studies showing the positive relationship between necrotic core tissue and RI in coronary [18] and renal arteries [3] to patients with carotid and iliac diseases. Our results suggest that coronary and peripheral artery diseases may share a common pathophysiological process with regard to plaque remodeling. In a postmortem study, a strong association was demonstrated between plaque and vessel area and inflammatory markers such as macrophages and T lymphocytes [19,20]. In a clinical study using VH-IVUS, Kubo et al. [21] demonstrated the association of percentage of necrotic core with elevated C-reactive protein, suggesting the relationship between necrotic core and inflammatory activity of the coronary atherosclerotic plaque.

In the current study, a variety of baseline characteristics was observed among different arteries. Varied contributions of risk factors to plaque development and progression in different arterial beds might explain heterogeneous patient characteristics among arteries at clinical presentation [22]. It is plausible that younger age could be associated with unstable plaque morphology in coronary artery disease [23]. In addition, unequal distribution of serum lipid levels and statin therapy observed among groups could be confounding factor as statin treatment changes plaque composition toward a more stable phenotype [24]. However, high proportion of statin use in patients with carotid artery disease might not account for the trend toward unstable phenotype in the carotid arteries and the same holds true for iliac artery disease. Thus, various underlying patient characteristics as well as regional differences might have influence on plaque morphology and disease expression in different arterial beds.

While the distribution of plaque phenotypes and composition in men and women was comparable, women were more likely to have higher remodeling index in carotid and renal artery in the current study. These trends are different from those in coronary arteries in which there was no gender difference regarding remodeling pattern [25]. These findings should be confirmed in a larger number of patients.

Although therapeutic aspects of the plaque characteristics in PAD were not covered in the current study, clinical implications of assessing plaque morphology were suggested for coronary intervention in which the underlining plaque characteristics are associated with the vascular response [26], distal embolism [27], and restenosis [28] after stent implantation. Further clinical studies are needed to address the question whether these observations hold true for PAD.

There are several limitations in this study. The study cohort was sampled from patients who had IVUS study. This fact holds the potential of selection bias. Then, IVUS images were acquired from the target lesion. Therefore, plaque phenotypes in other arterial beds in the same patient were not determined. This study would not answer the question of the interaction among arterial beds and the regional differences in disease expression under the influence of systemic factors in the same individual. As the IVUS pullback imaging was performed by manual pullback, longitudinal information was not obtained. In addition, VH-

IVUS has limited accuracy for detecting TCFA because of its low axial resolution (100–150 μm) to visualize a thin fibrous cap ($<65\mu\text{m}$) [29, 30]. Finally, validation study for VH-IVUS for renal and iliac artery has not established, although there is no reason to suspect that they would be different from the coronary or carotid artery techniques.

6. Conclusion

Atherosclerotic plaque phenotypes and composition were heterogeneous in four different arterial beds at clinical presentation; compared with coronary artery, renal and iliac arteries had more stable phenotypes. In contrast, the associations of remodeling pattern with plaque phenotype and composition were similarly observed among the various arterial beds. There is likely an underlying shared pathogenic mechanism of plaque remodeling. The current study also points to a potential underlying mechanism for the varied clinical presentation in different arterial beds.

References

1. Pasternak RC, Criqui MH, Benjamin EJ, et al. Atherosclerotic Vascular Disease Conference: Writing Group I: epidemiology. *Circulation*. 2004; 109:2605–2612. [PubMed: 15173042]
2. Dalager S, Paaske WP, Kristensen IB, Laurberg JM, Falk E. Plaque in superficial femoral arteries indicates generalized atherosclerosis and vulnerability to coronary death: an autopsy study. *Stroke*. 2007; 38:2698–2705. [PubMed: 17761918]
3. Kataoka T, Mathew V, Rubinshtein R, et al. Association of plaque composition and vessel remodeling in atherosclerotic renal artery stenosis: a comparison with coronary artery disease. *JACC Cardiovasc Imaging*. 2009; 2:327–338. [PubMed: 19356579]
4. Mintz GS, Nissen SE, Anderson WD, et al. American College of Cardiology Clinical Expert Consensus Document on Standards for Acquisition, Measurement and Reporting of Intravascular Ultrasound Studies (IVUS). A report of the American College of Cardiology Task Force on Clinical Expert Consensus Documents. *J Am Coll Cardiol*. 2001; 37:1478–1492. [PubMed: 11300468]
5. García-García HM, Mintz GS, Lerman A, et al. Tissue characterisation using intravascular radiofrequency data analysis: recommendations for acquisition, analysis, interpretation and reporting. *EuroIntervention*. 2009; 5:177–189. [PubMed: 20449928]
6. Takumi T, Mathew V, Barsness GW, et al. The association between renal atherosclerotic plaque characteristics and renal function before and after renal artery intervention. *Mayo Clin Proc*. 2011; 86:1165–1172. [PubMed: 22134935]
7. Kotani J, Mintz GS, Castagna MT, et al. Intravascular ultrasound analysis of infarct-related and non-infarct-related arteries in patients who presented with an acute myocardial infarction. *Circulation*. 2003; 107:2889–2893. [PubMed: 12782565]
8. Calvert PA, Obaid DR, O'Sullivan M, et al. Association between IVUS findings and adverse outcomes in patients with coronary artery disease: the VIVA (VHIVUS in Vulnerable Atherosclerosis) Study. *JACC Cardiovasc Imaging*. 2011; 4:894–901. [PubMed: 21835382]
9. Pentecost MJ, Criqui MH, Dorros G, et al. Guidelines for peripheral percutaneous transluminal angioplasty of the abdominal aorta and lower extremity vessels. A statement for health professionals from a special writing group of the Councils on Cardiovascular Radiology, Arteriosclerosis, Cardio-Thoracic and Vascular Surgery, Clinical Cardiology, and Epidemiology and Prevention, the American Heart Association. *Circulation*. 1994; 89:511–531. [PubMed: 8281692]
10. Okura H, Asawa K, Kubo T, et al. Incidence and predictors of plaque rupture in the peripheral arteries. *Circ Cardiovasc Interv*. 2010; 3:63–70. [PubMed: 20160185]
11. Janzen J, Lanzer P, Rothenberger-Janzen K, Vuong PN. The transitional zone in the tunica media of renal arteries has a maximal length of 10 millimetres. *Vasa*. 2000; 29:168–172. [PubMed: 11037713]
12. Janzen J, Lanzer P, Rothenberger-Janzen K, Vuong PN. Variable extension of the transitional zone in the medial structure of carotid artery tripod. *Vasa*. 2001; 30:101–106. [PubMed: 11417279]

13. Stroev PV, Hoskins PR, Easson WJ. Distribution of wall shear rate throughout the arterial tree: a case study. *Atherosclerosis*. 2007; 191:276–280. [PubMed: 16828101]
14. Samady H, Eshtehardi P, McDaniel MC, et al. Coronary artery wall shear stress is associated with progression and transformation of atherosclerotic plaque and arterial remodeling in patients with coronary artery disease. *Circulation*. 2011; 124:779–788. [PubMed: 21788584]
15. Mohler ER 3rd, Sarov-Blat L, Shi Y, et al. Site-specific atherogenic gene expression correlates with subsequent variable lesion development in coronary and peripheral vasculature. *Arterioscler Thromb Vasc Biol*. 2008; 28:850–805. [PubMed: 18276914]
16. Virmani R, Kolodgie FD, Burke AP, et al. Atherosclerotic plaque progression and vulnerability to rupture: angiogenesis as a source of intraplaque hemorrhage. *Arterioscler Thromb Vasc Biol*. 2005; 25:2054–2061. [PubMed: 16037567]
17. Hildebrandt HA, Gossel M, Mannheim D, et al. Differential distribution of vasa vasorum in different vascular beds in humans. *Atherosclerosis*. 2008; 199:47–54. [PubMed: 17959180]
18. Rodriguez-Granillo GA, Serruys PW, Garcia-Garcia HM, et al. Coronary artery remodelling is related to plaque composition. *Heart*. 2006; 92:388–391. [PubMed: 15964942]
19. Pasterkamp G, Schoneveld AH, Hijnen DJ, et al. Atherosclerotic arterial remodeling and the localization of macrophages and matrix metalloproteinases 1, 2 and 9 in the human coronary artery. *Atherosclerosis*. 2000; 150:245–253. [PubMed: 10856516]
20. Pasterkamp G, Schoneveld AH, van der Wal AC, et al. Relation of arterial geometry to luminal narrowing and histologic markers for plaque vulnerability: the remodeling paradox. *J Am Coll Cardiol*. 1998; 32:655–662. [PubMed: 9741507]
21. Kubo T, Matsuo Y, Hayashi Y, et al. High-sensitivity C-reactive protein and plaque composition in patients with stable angina pectoris: a virtual histology intravascular ultrasound study. *Coron Artery Dis*. 2009; 20:531–535. [PubMed: 19855269]
22. Faxon DP, Fuster V, Libby P, et al. Atherosclerotic Vascular Disease Conference: Writing Group III: pathophysiology. *Circulation*. 2004; 109:2617–2625. [PubMed: 15173044]
23. Hong YJ, Jeong MH, Ahn Y, et al. Age-related differences in intravascular ultrasound findings in 1,009 coronary artery disease patients. *Circ J*. 2008; 72:1270–1275. [PubMed: 18654012]
24. Nozue T, Yamamoto S, Tohyama S, et al. Statin treatment for coronary artery plaque composition based on intravascular ultrasound radiofrequency data analysis. *Am Heart J*. 2012; 163:191–199.e1. [PubMed: 22305836]
25. Lansky AJ, Ng VG, Maehara A, et al. Gender and the extent of coronary atherosclerosis, plaque composition, and clinical outcomes in acute coronary syndromes. *JACC Cardiovasc Imaging*. 2012; 5(3 Suppl):S62–S72. [PubMed: 22421232]
26. Hong YJ, Jeong MH, Kim SW, et al. Relation between plaque components and plaque prolapse after drug-eluting stent implantation--virtual histology-intravascular ultrasound. *Circ J*. 2010; 74:1142–1151. [PubMed: 20453386]
27. Kawamoto T, Okura H, Koyama Y, et al. The relationship between coronary plaque characteristics and small embolic particles during coronary stent implantation. *J Am Coll Cardiol*. 2007; 50:1635–1640. [PubMed: 17950143]
28. Okura H, Morino Y, Oshima A, et al. Preintervention arterial remodeling affects clinical outcome following stenting: an intravascular ultrasound study. *J Am Coll Cardiol*. 2001; 37:1031–1035. [PubMed: 11263604]
29. Sawada T, Shite J, Garcia-Garcia HM, et al. Feasibility of combined use of intravascular ultrasound radiofrequency data analysis and optical coherence tomography for detecting thin-cap fibroatheroma. *Eur Heart J*. 2008; 29:1136–1146. [PubMed: 18397871]
30. Kubo T, Nakamura N, Matsuo Y, et al. Virtual histology intravascular ultrasound compared with optical coherence tomography for identification of thin-cap fibroatheroma. *Int Heart J*. 2011; 52:175–179. [PubMed: 21646741]

Appendix A

Examples of angiographic and corresponding gray-scale intravascular ultrasound (IVUS). Ruptured plaques in left main coronary artery (A), internal carotid artery (B), renal artery

(C), and iliac artery (D). Arrowheads in angiographic images show target lesions. Gray-scale IVUS images show a cavity (asterisk) that communicated with the lumen and fibrous cap (arrows) overlaying a lipid core.

Appendix B

Examples of Plaque Phenotypes Classified by VH-IVUS. (A) virtual histology-intravascular ultrasound (VH-IVUS) thin-capped fibroatheroma (VH-TCFA) in coronary artery, (B) thick-capped fibroatheroma (VH-ThCFA) in carotid artery, (C) pathological intimal thickening (VH-PIT) in renal artery, and (D) fibrocalcific plaque (VH-FC) in iliac artery.

Appendix C. Gray-scale IVUS parameters

	Men	Women	P
Coronary artery	n=54	n=14	
Age, y	68±8	66±11	0.44
Lesion site			
EEM CSA, mm ²	20.7±4.5	16.8±6.0	0.008
P+M CSA, mm ²	13.7±4.5	10.6±4.4	0.03
Lumen CSA, mm ²	7.0±3.2	6.2±2.4	0.36
Plaque burden, %	65.6±13.6	62.5±8.4	0.42
Reference segment			
EEM CSA, mm ²	20.3±4.4	16.4±5.6	0.006
Remodeling index	1.04±0.15	1.07±0.15	0.50
Positive remodeling, n (%)	21 (39%)	8 (57%)	0.24
Plaque rupture, n (%)	9 (17%)	0 (0%)	0.19
Carotid artery	n=19	n=10	
Age, y	73±8	72±8	0.77
Lesion site			
EEM CSA, mm ²	40.2±12.4	39.9±17.3	0.96
P+M CSA, mm ²	32.9±10.1	29.9±16.7	0.54
Lumen CSA, mm ²	7.2±5.4	10.1±4.2	0.17
Plaque burden, %	82.4±9.7	71.5±14.9	0.03
Reference segment			
EEM CSA, mm ²	39.8±11.9	32.7±15.2	0.17
Remodeling index	1.02±0.19	1.25±0.23	0.007
Positive remodeling, n (%)	10 (53%)	7 (70%)	0.45
Plaque rupture, n (%)	1 (5%)	1 (10%)	1.00
Renal artery	n=30	n=20	
Age, y	71±9	72±8	0.90
Lesion site			
EEM CSA, mm ²	32.7±9.7	31.4±8.9	0.64
P+M CSA, mm ²	24.7±9.9	22.6±7.9	0.43
Lumen CSA, mm ²	8.4±5.4	8.8±3.8	0.77
Plaque burden, %	73.5±14.4	71.1±11.1	0.54
Reference segment			

	Men	Women	P
EEM CSA, mm ²	32.1±8.7	28.4±8.4	0.14
Remodeling index	1.03±0.19	1.13±0.23	0.12
Positive remodeling, n (%)	14 (47%)	12 (60%)	0.40
Plaque rupture, n (%)	1 (3%)	2 (10%)	0.56
Iliac artery	n=10	n=4	
Age, y	67±13	82±8	0.06
Lesion site			
EEM CSA, mm ²	52.6±38.1	53.0±15.7	0.99
P+M CSA, mm ²	23.0±7.3	27.7±7.2	0.84
Lumen CSA, mm ²	22.5±18.7	25.2±11.6	0.79
Plaque burden, %	61.3±20.0	54.0±12.1	0.51
Reference segment			
EEM CSA, mm ²	57.9±41.4	52.3±14.0	0.80
Remodeling index	0.93±0.13	1.02±0.21	0.34
Positive remodeling, n (%)	4 (40)	1 (25)	1.00
Plaque rupture, n (%)	1 (10)	0 (0)	1.00

CSA indicates cross-sectional area; EEM, external elastic membrane, and P+M, plaque plus media.

Appendix D. Virtual histology IVUS parameters

	Men	Women	P
Coronary artery	n=54	n=14	
Phenotype			
VH-TCFA	16 (30)	6 (43)	0.60
VH-ThCFA	9 (17)	3 (21)	
VH-PIT	11 (20)	1 (7)	
VH-FC	18 (33)	4 (29)	
Composition			
Fibrous plaque area (%)	56 [46,65]	52 [41,73]	0.83
Fibro-fatty plaque area (%)	16 [11,28]	16 [11,32]	0.98
Necrotic core plaque area (%)	16 [13,23]	14 [9,29]	0.56
Dense calcium plaque area (%)	6 [2,12]	5 [1,10]	0.67
Carotid artery	n=19	n=10	
Phenotype			
VH-TCFA	4 (21)	3 (30)	0.43
VH-ThCFA	4 (21)	2 (20)	
VH-PIT	4 (21)	4 (40)	
VH-FC	7 (37)	1 (10)	
Composition			
Fibrous plaque area (%)	59 [50,62]	59 [56,69]	0.25
Fibro-fatty plaque area (%)	25 [10,37]	18 [15,26]	0.60

	Men	Women	P
Necrotic core plaque area (%)	11 [9, 20]	15 [9, 21]	0.48
Dense calcium plaque area (%)	3 [1,7]	2 [1,7]	0.51
Renal artery	n=30	n=20	
Phenotype			
VH-TCFA	5 (17)	3 (15)	0.53
VH-ThCFA	3 (10)	0 (0)	
VH-PIT	17 (57)	13 (65)	
VH-FC	5 (17)	4 (20)	
Composition			
Fibrous plaque area (%)	60 [50, 68]	59 [53, 64]	0.71
Fibro-fatty plaque area (%)	25 [14,36]	26 [15,34]	0.80
Necrotic core plaque area (%)	6 [4,15]	10 [4, 16]	0.60
Dense calcium plaque area (%)	3 [0, 6]	4 [1, 9]	0.20
Iliac artery	n=10	n=4	
Phenotype			
VH-TCFA	1 (10)	0 (0)	0.80
VH-ThCFA	0 (0)	0 (0)	
VH-PIT	4 (40)	2 (50)	
VH-FC	5 (50)	2 (50)	
Composition			
Fibrous plaque area (%)	55 [35,60]	53 [35, 60]	0.73
Fibro-fatty plaque area (%)	20 [13,36]	26 [9,49]	0.84
Necrotic core plaque area (%)	16 [8, 24]	12 [10,20]	0.64
Dense calcium plaque area (%)	11 [3, 15]	8 [6,12]	0.84

VH-TCFA indicates thin-capped fibroatheroma; VH-ThCFA, thick-capped fibroatheroma; VH-PIT, pathological intimal thickening; and VH-FC, fibrocalcific plaque.

- Compared to coronary arteries, fibroatheroma was less frequently observed in renal and iliac arteries.
- Positive remodeled lesions demonstrated more fibroatheroma in coronary, carotid, and renal arteries.
- There was positive relationship between remodeling index and percent necrotic area in all four arteries.

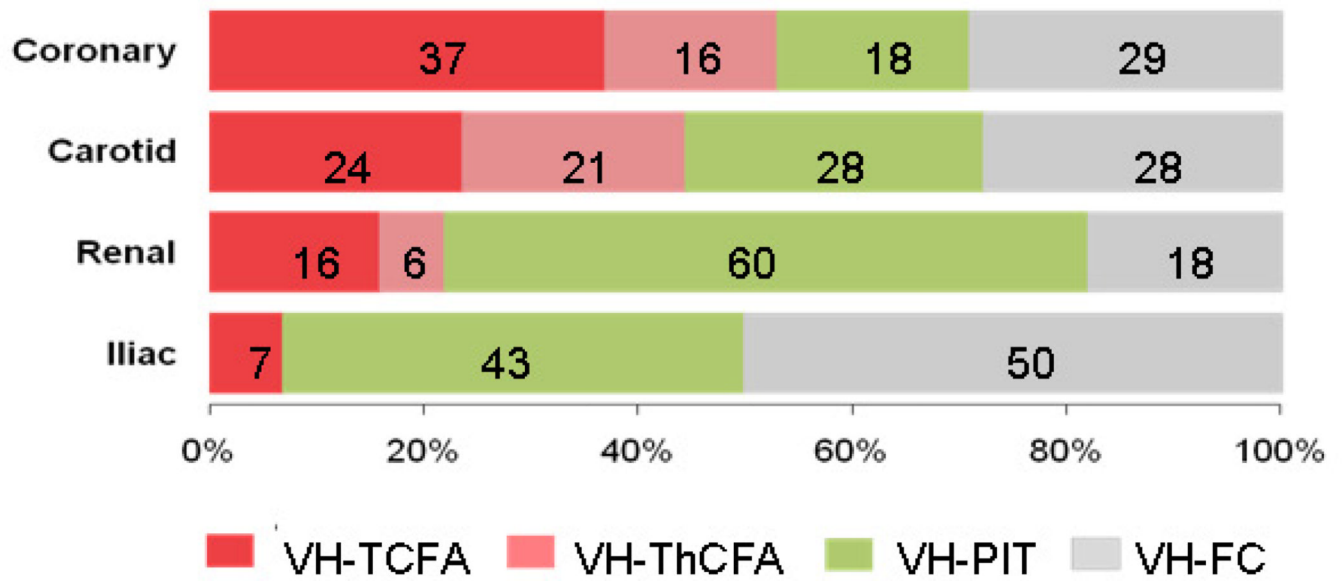


Figure 1.

The frequencies of plaque phenotypes in each vasculature. The distribution of plaque phenotypes was different among four vascular beds ($P < 0.001$). Plaques demonstrated less characteristics of VH-FA (both VH-TCFA and VH-ThCFA) in renal ($p < 0.001$ vs. coronary) and iliac arteries ($p = 0.006$ vs. coronary). VH-FA= fibroatheroma; VH-TCFA= thin-capped fibroatheroma; VHThCFA= thick-capped fibroatheroma; PIT= pathological intimal thickening; and VH-FC= fibrocalcific plaque.

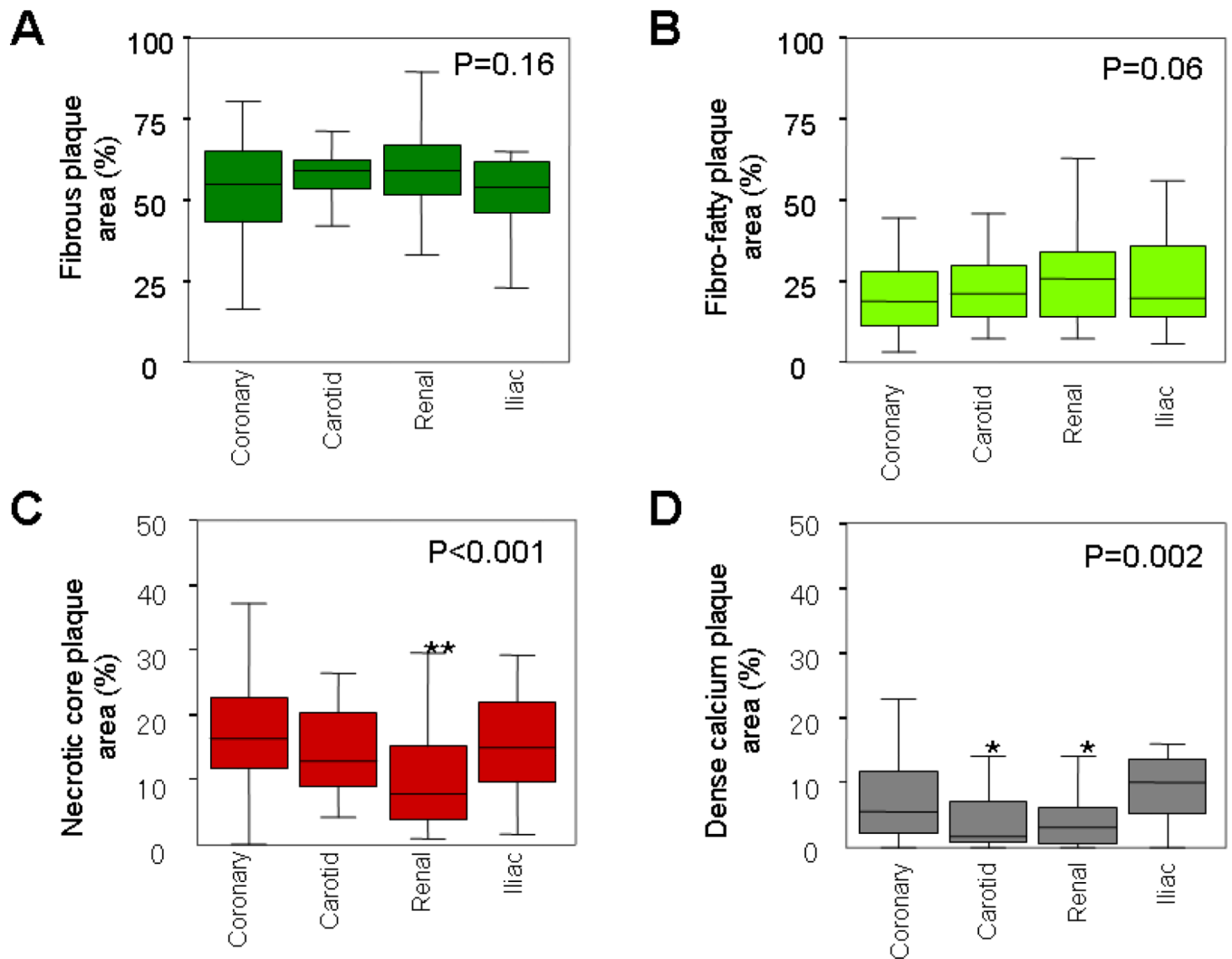
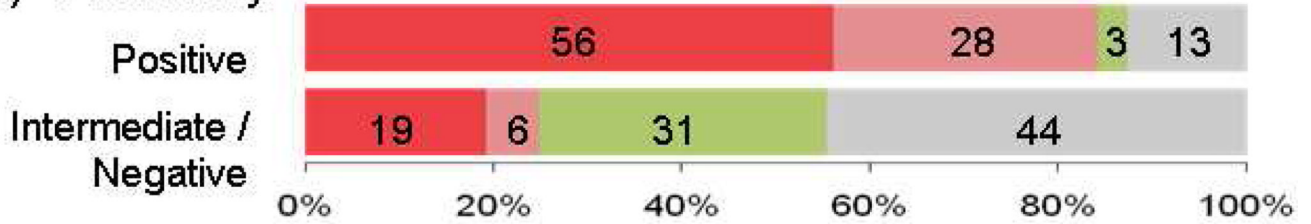
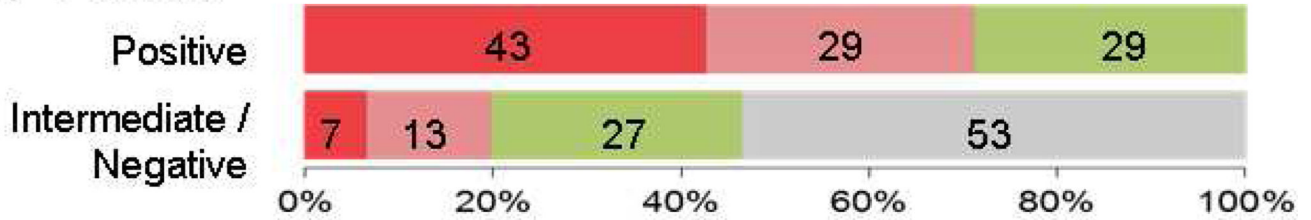


Figure 2. Plaque composition at the smallest lumen site in four arteries. Box-whisker plots displayed the percent area of (A) fibrous plaque, (B) fibro-fatty plaque, (C) necrotic core, and (D) dense calcium of the whole plaque area. Renal arteries had less percentage of necrotic core (** $p < 0.001$ vs. coronary). Carotid (* $p = 0.04$ vs. coronary) and renal arteries (* $p = 0.01$ vs. coronary) had less percentage of dense calcium.

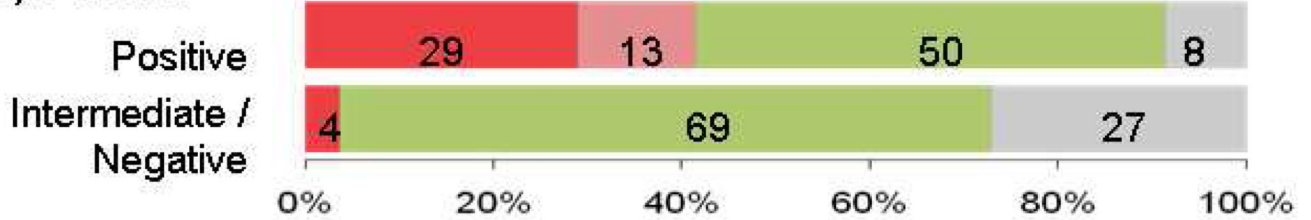
(A) Coronary



(B) Carotid



(C) Renal



(D) Iliac

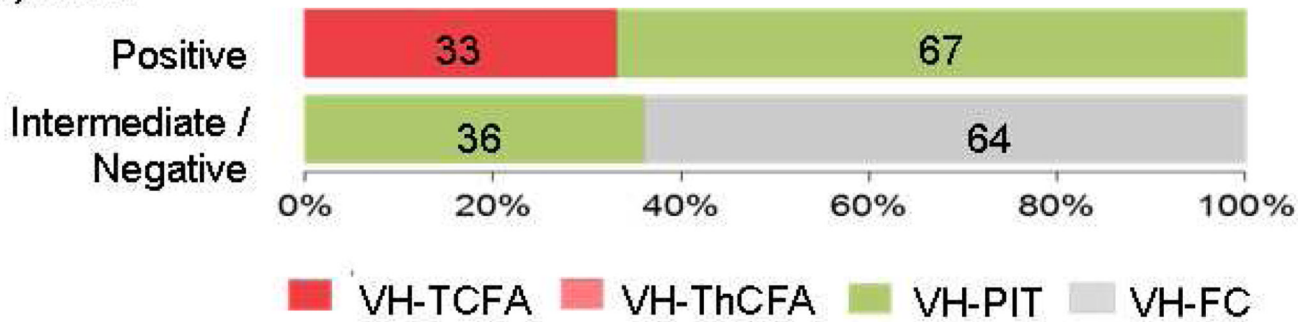


Figure 3.

The distributions of plaque phenotypes stratified by remodeling mode in four arteries. The distributions of plaque phenotypes were different between positive and intermediate/negative remodeled lesions in coronary ($p < 0.001$), carotid ($p = 0.01$), renal ($p = 0.01$), and iliac arteries ($p = 0.04$). Compared to intermediate/negative remodeled lesions, positive remodeled lesions demonstrated more characteristics of VH-FA (VH-TCFA and VH-ThCFA) in coronary (84% vs. 25%, $p < 0.001$), carotid (72% vs. 20%, $p = 0.001$), and renal arteries (42% vs. 4%, $p = 0.001$). VH-FA= fibroatheroma; VH-TCFA= thin-capped fibroatheroma; VH-ThCFA= thick-capped fibroatheroma; VH-PIT=pathological intimal thickening; and VH-FC=fibrocalcific plaque.

Table 1

Patient Characteristics

	Coronary artery (n=68)	Carotid artery (n=29)	Renal artery (n=50)	Iliac artery (n=14)	P
Age, y	68±9	73±8	71±9	71±14	0.04
Male	54 (79)	19 (66)	30 (60)	10 (71)	0.14
Hypertension	56 (82)	29 (100)*	48 (96)	13 (93)	0.02
Dyslipidemia	52 (76)	27 (93)	41 (82)	12 (86)	0.27
Diabetes	23 (34)	10 (34)	21 (42)	7 (50)	0.60
Current smoking	12 (18)	6 (21)	10 (20)	3 (21)	0.98
LDL cholesterol, mg/dL	85±26	85±31	94±42	86±28	0.47
HDL cholesterol, mg/dL	46±11	45±9	46±12	44±15	0.96
Triglycerides, mg/dL	127±53	184±73	178±212	139±66	0.09
Total cholesterol, mg/dL	152±38	166±38	175±75	156±31	0.11
Creatinine, mg/dL	1.1±0.4	1.1±0.3	1.2±0.5	1.3±0.9	0.09
Statin therapy	53 (76)	28 (97)	53 (76)	8 (57)	0.02

HDL indicates high-density lipoprotein; ICE, ischemic cardiac events; LDL, low-density lipoprotein; and PAD, peripheral artery disease.

* p<0.0167 vs. coronary artery.

Table 2

Gray-scale IVUS Parameters of Culprit Lesions in Four Arteries

Lesion site	coronary	carotid	renal	iliac	P
EEM CSA, mm ²	19.9±5.1	40.1±14.0*	32.2±9.3*	52.7±32.6*	<0.001
P+M CSA, mm ²	13.1±4.6	31.9±12.5*	23.9±9.1*	29.5±19.5*	<0.001
Lumen CSA, mm ²	6.9±3.0	8.3±5.1	8.6±4.8	23.3±16.5*	<0.001
Plaque burden, %	65±13	79±13*	73±13*	59±18	<0.001
Reference segment					
EEM CSA, mm ²	19.5±4.9	37.4±13.3*	30.6±8.7*	56.3±35.2*	<0.001
Lumen CSA, mm ²	13.5±4.0	26.4±11.3*	22.7±7.8*	44.1±30.8*	<0.001
P+M CSA, mm ²	6.0±2.8	11.0±7.8*	7.9±3.9*	12.2±7.8*	<0.001
Plaque burden, %	30.4±11.7	29.2±16.1	26.5±11.7	24.2±13.1	0.23
Remodeling index	1.05±0.14	1.09±0.22	1.08±0.20	0.95±0.16	0.09
Positive remodeling, n (%)	29 (43)	17 (59)	26 (52)	5 (36)	0.59
Plaque rupture, n (%)	9 (13)	2 (7)	3 (6)	1 (7)	0.54

CSA indicates cross-sectional area; EEM, external elastic membrane, and P+M, plaque plus media.

* p<0.0167 vs. coronary arter